Order-N spectral method for electromagnetic waves

C.T. Chan, Q.L. Yu, and K.M. Ho
Ames Laboratory–United States Department of Energy and Department of Physics and Astronomy, Iowa State University, Ames, Iowa 50011
(Received 12 December 1994)

We show that the eigenmodes for electromagnetic waves in an inhomogeneous dielectric medium can be obtained with an algorithm that scales linearly with the size of the system. The method employs discretization of the Maxwell equations in both the spatial and the time domain and the integration of the Maxwell equations in the time domain. The spectral intensity can then be obtained by a Fourier transform. We applied the method to a few problems of current interest, including the photonic band structure of a periodic dielectric structure, the effective dielectric constants of some three-dimensional and two-dimensional systems, and the defect states of a periodic dielectric structure with structural defects.

I. INTRODUCTION

In the past few years, there has been much interest in the "photonic band gap" problem,[1] which is concerned with the existence of a frequency gap in the electromagnetic (EM) wave spectrum. It has been demonstrated by both theory and experiments that such a spectral gap can be realized[2] in a certain class of inhomogeneous periodic dielectric media, which are called "photonic crystals." Within a few years, we have witnessed rather rapid progress in this field, and theory has played an important role in providing accurate and timely solutions to this class of problem. In theoretical terms, we are basically solving the Maxwell equations for an inhomogeneous and periodic medium. The close analogy between the EM wave problem and the electronic structure problem has been noted and emphasized by many authors. In some aspects, the EM wave problem is easier to handle, mainly because we need to deal with a strongly interacting many-body problem for the electronic structure problem, whereas the EM wave problem (as described by the Maxwell equations) can be solved to arbitrary accuracy if a good numerical algorithm is available. Comparison with experimental results is also more direct for the case of EM waves. On the other hand, there are some complexities that are specific to the EM wave problem: the topology of the dielectric structure can be very complicated, the dielectric constant can be complex and frequency dependent, and EM waves must be treated as vector waves. Nevertheless, it is fair to say that instead of inventing new methods for the EM wave problem, what we have been doing is to adapt well tested methods in electronic structure calculations to the electromagnetic wave problem. For example, the plane wave method[3] and the Korringa-Kohn-Rostoker (KKR) method[4] are popular methods in electronic structure calculations. The formalism introduced by Pendry and MacKinnon[5] and Stefanou *et al.*[6] bears some similarity to the theory of low-energy electron diffraction. The "operator" algorithm of Meade *et al.*[7] is also frequently used in modern large scale electronic structure calculations that employ plane wave basis sets. For the electronic structure problem, the complexity of the traditional schemes scales like N^3, where N is proportional to the size of the system. The reason is that we usually employ a basis expansion and transform the electronic structure problem into an eigenvalue problem of the form $H\psi = e\psi$, and diagonalizing a Hermitian matrix H needs $O(N^3)$ operations. Such standard N^3 methods have served us well for ideal systems with small unit cells, but the prospect of handling complex and big systems is dim even with supercomputers. That is why there has recently been a flurry of activities to devise new methods that scales more favorably with the system size, and it has now been demonstrated that electronic structure calculations can, in principle, be treated with a computation effort that scales linearly with the size of the system.[8] These methods are called order-N methods. The main purpose of the present article is to demonstrate that the EM wave problem can also be solved with an order-N algorithm. The formulation of order-N methods is important, not only because they couple well with modern multiprocessor computers (parallel machines), but also because for large enough systems it is the "power law" that eventually dominates. For the particular case of the photonic band gap problem, the photonic bands for a perfect photonic crystal can be handled well by the plane wave method. However, in many plausible applications of such material, structures with controlled defects or structures with a certain degree of disorder may perhaps be more important than the ideal periodic structure. The defect structures can still be modeled with giant supercells, but for those complex systems the computational effort and the memory requirement become excessive if we use traditional N^3 methods. We are thus motivated to search for alternate algorithms that scale better with the system size.

This paper will be organized as follows. In Sec. II, we will outline the computation scheme. In Sec. II, the photonic bands of a photonic crystal with the symmetry of the diamond crystal structure is presented. In Sec. III, we will show that the effective dielectric constants of some complex three- and two-dimensional (3D and 2D)

structures can be obtained with the present method. We will obtain the defect states of a periodic dielectric structure with a structural defect in Sec. IV; and some remarks will be given in Sec. V.

II. METHOD OF CALCULATION

Let us consider the Maxwell equations

$$\nabla \times \mathbf{E} = -\frac{\partial \mathbf{H}}{\partial t}, \quad \nabla \times \mathbf{H} = \epsilon(\mathbf{r})\frac{\partial \mathbf{E}}{\partial t}, \tag{1}$$

where $\epsilon(\mathbf{r})$ is a position dependent dielectric constant. Once the boundary conditions and the initial conditions are specified, we can solve for the normal modes by discretizing both in space and time. When the fields are specified at an instant t=0, the spatial derivatives and hence the curls of the fields can be determined, most conveniently using finite differences. The Maxwell equations [Eq. (1)] then give us the time derivative of the fields which allow us to update the $\mathbf{H}(\mathbf{r},t)$ and $\mathbf{E}(\mathbf{r},t)$ fields in the time domain. The fields $\mathbf{H}(\mathbf{r},t)$ and $\mathbf{E}(\mathbf{r},t)$ can then be recorded as a time series for some sampling points in the system,[9] and, for a sufficiently large number of time steps (which governs the resolution in the frequency domain), the time series are Fourier (Laplace) transformed to the frequency domain to obtain the spectral intensities $g_{j,\alpha}(\omega) = \int dt\ e^{-i\omega t}\langle \phi_\alpha(\mathbf{r}_j,t)\phi_\alpha(\mathbf{r}_j,0)\rangle = |\phi^{(\omega)}_{j,\alpha}|^2$, where $\phi_{j,\alpha}$ is the α component of the fields $\mathbf{E}(\mathbf{r}_j)$ or $\mathbf{H}(\mathbf{r}_j)$ at point $\mathbf{r}_j$. This is equivalent to obtaining the spectral intensity by getting the Fourier transform of the field-field autocorrelation function, and is basically the same technique frequently used to obtain phonon frequencies by velocity-velocity correlation functions in classical molecular dynamics. The peaks in the spectra in the frequency domain give us the frequencies of the normal modes. The development of the present method is strongly motivated by similar methods for electrons[10] as well as the generation of phonon frequency using classical molecular dynamics techniques.[11] This method also falls into the category of algorithms called "finite-difference time-domain" methods in the electrical engineering community.[12]

A. The spatial derivatives

The $\mathbf{E}$ and the $\mathbf{H}$ fields are defined on a uniform grid and the spatial derivatives are calculated using the simple finite difference formulas. For example, the curls are determined by the spatial derivatives of the form $d\mathbf{E}_\alpha/d\beta$, where α and β are the x, y, z components, and these derivatives are determined by formulas such as $dE_x(i,j,k)/dy = [E_x(i,j+1,k) - E_x(i,j-1,k)]/2d$, where d is the distance between adjacent grid points. If possible, the discretization in the numerical algorithm should be chosen to satisfy the "conservation laws." We can define a total energy of the electromagnetic fields of the form

$$E_{\rm tot} = (1/8\pi)\int d^3r(\epsilon \mathbf{E}\cdot\mathbf{E}^* + \mathbf{H}\cdot\ \mathbf{H}^*). \tag{2}$$

It is straightforward to show that $dE_{\rm tot}/dt = 0$, if the spatial derivatives are computed exactly. It is interesting to note that, even when the spatial derivatives are evaluated with the finite difference equations, energy conservation still holds. In principle, the spatial derivatives can be calculated to the full precision allowed by the grid using fast Fourier transforms, at the expense of using more operations per time step.[13]

B. Time integration

The numerical time integration is performed by a fourth-order predictor-corrector approach (Adams-Bashforth-Moulton).[14] We are limited by two factors in the numerical time integration, the total time and the time interval of each time step. The total time (T) used in the simulation limits the lowest frequency that can be simulated to approximately $\omega_{\rm min} \sim 2\pi/T$, and also limits the frequency resolution to the same order of magnitude. The size of the time step (t) is directly related to the accuracy of the numerical integration and it also limits the highest frequency that can be simulated to approximately $\omega_{\rm max} \sim 2\pi/t$. There is an unavoidable error due to the time integration using a finite step size in the numerical algorithms, so that $E_{\rm tot}(t+dt)$ is not equal to $E_{\rm tot}(t)$. This error provides a good criterion for choosing the size of the time step. The fourth-order predictor-corrector algorithm performs well and we choose our time step such that the total energy is conserved to about 1% for the complete simulation.

C. Boundary conditions

The method basically solves coupled first-order differential equations in a finite spatial domain, so we must specify the boundary conditions. In this paper, we will be mainly concerned with periodic boundary conditions. There are two ways in which we can impose periodic boundary conditions in our simulation. For a periodic system, the fields can be written in the Bloch form [i.e., $\mathbf{H}(\mathbf{r}) = e^{i\mathbf{k}\cdot\mathbf{r}}\mathbf{h}(\mathbf{r})$, $\mathbf{E}(\mathbf{r}) = e^{i\mathbf{k}\cdot\mathbf{r}}\boldsymbol{\xi}(\mathbf{r})$, and $\mathbf{h}(\mathbf{r})$ and $\boldsymbol{\xi}(\mathbf{r})$ are periodic]. Then Eq. (1) can be rewritten as

$$i\mathbf{k}\times\boldsymbol{\xi} + \nabla\times\boldsymbol{\xi} = -\frac{\partial \mathbf{h}}{\partial t}, \quad i\mathbf{k}\times\mathbf{h} + \nabla\times\mathbf{h} = \epsilon(\mathbf{r})\frac{\partial \boldsymbol{\xi}}{\partial t}, \tag{3}$$

and the simulations can be performed on the reduced fields $\boldsymbol{\xi}(\mathbf{r})$ and $\mathbf{h}(\mathbf{r})$ within the unit cell. Another way is to impose the periodic boundary condition explicitly on $\mathbf{E}(\mathbf{r})$ and $\mathbf{H}(\mathbf{r})$ across the unit cells. In this case, we require that the fields in the adjacent unit cell satisfy $\mathbf{E}(\mathbf{r}+\mathbf{L}) = e^{i\mathbf{k}\cdot\mathbf{L}}\mathbf{E}(\mathbf{r})$ where $\mathbf{L}$ is the lattice vector. With the finite difference approach, it is more economical to work with the explicit imposition since it involves fewer mathematical operations.

D. The initial condition

The initial condition depends on the particular problem we want to study, and it can be a plane wave if we want a dispersion relation, or random fields if we want the density of states. They will be discussed below. An important requirement is that the initial field must have nonzero projections on the normal modes we are interested in.

E. Scaling

The complexity of the present method scales like $T \sim N_t \times N_{\text{grid}}$, where T is the total time needed to perform a calculation, N_t is the total number of time steps, and N_{grid} is the number of real space grid points used. The total number of time steps used controls the frequency resolution, and also the lowest frequency that can be simulated. We note that for most physical problems the upper and lower frequencies of interest and the frequency resolution do not change with the size of the system under consideration. For example, let us start with a perfect periodic system and suppose that it has a spectral gap, and we introduce a defect, expecting to find defect states in the gap. The existence of the defect certainly mandates a much bigger cell to simulate. However, the spectral width of interest remains the same so that N_t remains the same. We only need to increase the number of grid points N_{grid}, which is proportional to the size of system under consideration, so that this method scales like N^1. The memory required also scales linearly with the size of the systems. The algorithm is very suitable for parallel machines, especially when finite differences are used. Most of the numerical calculations presented below are performed on parallel machines (N cube and Paragon).

III. PHOTONIC BAND FOR A DIAMOND STRUCTURE

We calculated the photonic band dispersion for a photonic crystal using the present method. The photonic crystal has the symmetry of a diamond structure[15] and is constructed with dielectric cylinders ($\epsilon = 12.96$) connecting the nearest neighbor lattice points in a diamond lattice. The dielectric cylinders have circular cross sections and they occupy 20% of the volume in the structure. Such structures have been shown to possess full photonic band gaps. The photonic bands of this structure are found with the present method and plotted in Fig. 1, and compared with the results generated from the plane wave expansion method, which is the most popular method for photonic band calculations.[3] The results for the plane wave methods are obtained by expanding the wave functions with about 1000 plane waves per $\mathbf{k}$ point (i.e., diagonalizing 2000×2000 matrices due to the vector wave nature of light). The agreement is very good. In this simulation, we used the staggered grid,[16] and the cubic conventional cell is defined by a grid of $48\times48\times48$ points.

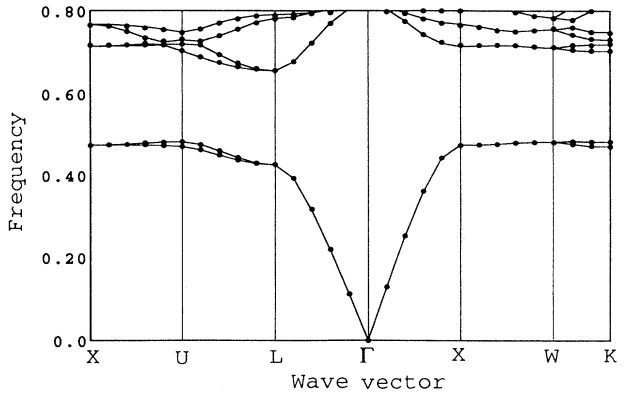

FIG. 1. The photonic bands of a diamond structure generated with the spectral method (dots) compared with the plane wave method (lines). The frequencies are in units of c/a, where c is the speed of light and a is the lattice constant.

Each "grid point" is actually regarded as a cell containing $30\times30\times30$ points, and the dielectric constant of the grid point is taken to be the average dielectric constant of the subcell, which means that for the points close to the boundary of the cylinders its value is somewhere between 1 and 12.96. We used a total of 100 000 time steps in the simulation, with each time step $0.003a/c$, where a is the lattice constant and c is the velocity of light. We will use a/c as time units throughout the paper, and angular frequencies (ω) are measured in units of $2\pi\frac{c}{a}$. The initial condition (the fields at $t = 0$) is chosen such that $\mathbf{E}(\mathbf{r})=0$ and $\mathbf{H}(\mathbf{r}) = \sum_{\mathbf{G}} \mathbf{h}_0(\mathbf{k}+\mathbf{G})e^{i(\mathbf{k}+\mathbf{G})\cdot\mathbf{r}}$, where $\mathbf{k}$ is the $\mathbf{k}$ vector under consideration and $\mathbf{h}_0(\mathbf{k}+\mathbf{G}) = \mathbf{v}\times(\mathbf{k}+\mathbf{G})$,[17] with $\mathbf{v}$ chosen to be a vector such that its x, y, z components are of roughly equal magnitude. Such a choice of initial condition guarantees that $\mathbf{H}$ satisfies $\nabla\cdot\mathbf{H} = 0$. Note that if the initial $\mathbf{H}$ field is transverse it will remain transverse in the course of the simulation. This procedure filters out the longitudinal modes of the Maxwell equations which have $\omega = 0$ and shows no dispersion. $\mathbf{H}(\mathbf{r}_i, t)$ is recorded for 64 evenly (but randomly) chosen points in the unit cell, and $H_{x,y,z}(\mathbf{r}_i, \omega)$ is obtained by Fourier transform, and similarly for $E_{x,y,z}(r_i, \omega)$. The spectral intensities of all 64 points are then added up together to identify the eigenmodes.[18] Figure 2 shows the spectral intensities at the X point. We note that different eigenmodes do not mix their energies during the simulation, so that the magnitude of the peaks in the spectral intensity depends on the initial field at t=0. Only the positions of the peaks are meaningful.

IV. EFFECTIVE DIELECTRIC CONSTANTS

This method can be used to obtain the effective dielectric constants of an inhomogeneous medium. The effective dielectric properties of a multicomponent system have been studied for nearly a century,[19] and it is a very difficult mathematical problem. Effective medium approximations such as the Bruggeman[20] and Maxwell-

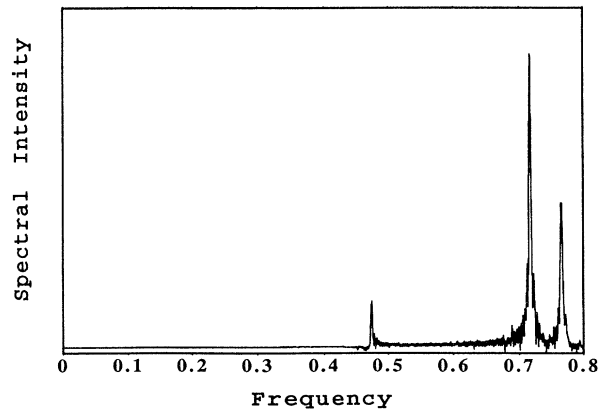

FIG. 2. Spectral intensity at the X point of the diamond structure.

Garnett[21] theories have been known for a long time and they can give rather reasonable results if the underlying assumption (spherical objects in an effective medium) is good for the situation under study. For example, the Maxwell-Garnett theory is good for isolated spherical objects in an otherwise uniform medium, while symmetric Bruggeman theories work best for multicomponent systems where different components are equal in importance. These effective medium theories in general neglect the microstructure of inhomogeneous media and the results are determined solely by the filling ratio or the concentration of the individual components. There are also analytical theories that give upper and lower bounds of the effective ϵ.[22] Recently, numerical algorithms have been formulated that can in principle calculate the effective dielectric constants exactly for systems with *arbitrary* shape, and these methods are usually Fourier space methods, and are applicable to simple, ordered, and periodic systems.[23] These methods typically scale like N^3, since they need to invert a matrix or solve a system of equations. For structures with sharp boundaries, it is rather difficult to converge the results with Fourier space (plane wave) methods, and extrapolation is frequently required to obtain the correct result. These numerical methods are useful for man-made simple composites but are of limited use in treating composite materials that exist in nature, which usually have fairly disordered microstructures. For inhomogeneous systems that are not ordered, or are "complex" in microstructure, the effective dielectric constants are very difficult to obtain, and the present method may prove useful.

The effective dielectric constant can be obtained with the present method in the following manner. In the wavelength limit, the dispersion relation is linear, obeying the relation $n\omega = ck$; and hence $\epsilon = \lim_{k\to\text{small}} (\frac{ck}{\omega})^2$. The effective ϵ in any direction for an arbitrary object can then be found by setting an initial field to be a plane wave with wave vector $\mathbf{k}$ with $\mathbf{H}(\mathbf{r}) = \boldsymbol{\eta} e^{i\mathbf{k}\cdot\mathbf{r}}$, where $\frac{\mathbf{k}}{|\mathbf{k}|}$ is small, and $\boldsymbol{\eta}$ is just a constant vector normal to $\mathbf{k}$. We can also use random fields as long as we impose the periodic boundary conditions explicitly according to the wave vector $\mathbf{k}$ we have chosen. However, it is usually advantageous to use a plane wave with constant coefficients since random initial fields have high-frequency components that require a small time step to conserve the total energy of the system. In principle, the smaller the magnitude of $\mathbf{k}$ the better, but in practice too small a $\mathbf{k}$ will give numerical problems. Typical values of $|\mathbf{k}|$ used vary from $0.05\frac{2\pi}{a}$ to $0.1\frac{2\pi}{a}$ in the following calculations. The number of time steps (N_t) used must be larger than $N_t = 2\pi\sqrt{\epsilon}/(ckt)$, where t is the size of the time step. [We of course do not know ϵ before the calculation, but we do know that ϵ is always bounded above by the volume average of $\epsilon(\mathbf{r})$.] The number of time steps we used in the following examples is substantially larger than this estimate and will be specified below. The calculations are more demanding for systems with higher dielectric constants, and we believe that this is inevitable with any numerical formulation for the effective dielectric constant problem. In the following, we will present some calculations for 3D and 2D systems. We will consider both ordered and randomly tiled systems. For randomly tiled systems, we will use the term "normalized standard deviation" to refer to the quantity $\int d\mathbf{r}[\epsilon(\mathbf{r}) - \langle\epsilon\rangle]^2/\langle\epsilon\rangle^2$, and the volume (or area) averaged ϵ will be denoted by $\langle\epsilon\rangle$.

A. Three dimension

1. *Ordered structures*

In the first test, we calculated the effective dielectric constant of a periodic system of dielectric spheres ($\epsilon = 3$) arranged in a simple cubic lattice as a function of the filling ratio of the spheres. The spheres are overlapping when the filling ratio exceeds 52%. In the simulation, we used a 48×48×48 grid in the unit cell, and a total of 60 000 time steps, with each step being $0.004a/c$ units. The initial fields correspond to the $\mathbf{k}$ vector $(0.1,0,0)2\pi/a$. In Fig. 3, our results are compared with those of Bergman and Dunn,[23] and the agreement is very good.

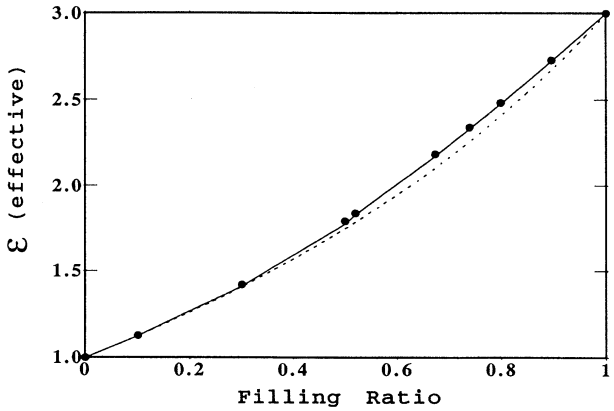

FIG. 3. The effective dielectric constants of dielectric spheres ($\epsilon = 3$) arranged in a cubic lattice as a function of filling ratio of the spheres, calculated with the spectral method (dots), and compared with Bergman and Dunn's results (solid line). The dotted line is the Maxwell-Garnett result.

2. Disordered structures

We randomly tiled a 3D 48×48×48 grid such that each point has an $\epsilon(\mathbf{r})$ generated by a random-number generator with a volume average $\epsilon \sim 25$, and the normalized standard deviation $\sim 1/3$. We made two runs. For the first run, $\langle\epsilon\rangle$ =25.035 61 and the normalized standard deviation = 0.326 23, and we ran 350 000 time steps with each time step $0.002a/c$ units. The plane wave used has $\mathbf{k}$=(0.05,0.0,0.0)$\frac{2\pi}{a}$. The effective ϵ is found to be 21.96. For the second run, a different seed was used for the random-number generator, and we used a plane wave with $\mathbf{k}$=(0.1,0.0,0.0)$\frac{2\pi}{a}$, a time step of $0.0015a/c$, and a total of 1 500 000 time steps. In this run, $\langle\epsilon\rangle = 24.9316$ and the normalized standard deviation is 0.330 73, and the effective ϵ is found to be 21.86.

For both runs, $\epsilon_{\text{eff}}/\langle\epsilon\rangle = 0.877$. According to the theory of Herring,[24] $\epsilon_{\text{eff}}/\langle\epsilon\rangle = 1 - \frac{1}{3}\int d\mathbf{r}[\epsilon(\mathbf{r}) - \langle\epsilon\rangle]^2/\langle\epsilon\rangle^2$, up to second order in the normalized standard deviation for an isotropic system; which is 0.89 for both cases. Although the Herring formula is a second-order expansion and is not intended for small normalized standard deviation, the current results show that it works reasonably well even in this test case of moderately large standard deviation.

We also studied a 3D random two-component "checkerboard" system, which has a 48×48×48 grid, with each grid point having a dielectric constant of either 5 or 15 with equal probability (as decided by a random-number generator). We make two simulations. In the first run, the $\langle\epsilon\rangle$ is 9.9904 and the normalized standard deviation is 0.250 48. We used a plane wave with wave vector (0.05,0.05,0.05)$\frac{2\pi}{a}$ and a time step of $0.0015a/c$ units, and a total of 600 000 steps. The effective ϵ is found to be 9.10. The second run has $\langle\epsilon\rangle$= 10.011 with a normalized standard deviation of 0.2495, and we run for 800 000 steps. ϵ is found to be 9.124. The ratio $\epsilon_{\text{eff}}/\langle\epsilon\rangle$ is 0.911 for both cases. Herring's formula gives (up to second order in the normalized standard deviation) $\epsilon_{\text{eff}}/\langle\epsilon\rangle = 0.917$, again in reasonable agreement with the numerical result. For this particular case, the Hashin-Shtrikman theorem bounds the effective ϵ between the values $0.875 < \epsilon_{\text{eff}}/\langle\epsilon\rangle < 0.9375$, and Bruggeman theory gives $\epsilon_{\text{eff}}/\langle\epsilon\rangle = 0.9114$.

B. Two dimension

In two dimensions, the situation is somewhat simpler. The Maxwell equations decouple into an E_z-polarized (TM) mode and an H_z-polarized (TE) mode. For the E_z-polarized mode, the $\mathbf{E}$ and the $\mathbf{H}$ fields are, respectively, $\mathbf{E}(\mathbf{r}) = (0,0,E)$ and $\mathbf{H}(\mathbf{r}) = (H_x, H_y, 0)$ and the Maxwell equations become

$$\frac{\partial E}{\partial x} = \frac{dH_y}{dt}, \quad \frac{\partial E}{\partial y} = -\frac{dH_x}{dt}, \quad \frac{\partial H_y}{\partial x} - \frac{\partial H_x}{\partial y} = \epsilon\frac{dE}{dt}, \tag{4}$$

which is equivalent to

$$\frac{\partial^2 E}{\partial x^2} + \frac{\partial^2 E}{\partial y^2} = \epsilon\frac{d^2E}{dt^2}. \tag{5}$$

The H_z-polarized mode has $\mathbf{H}(\mathbf{r}) = (0,0,H)$ and $\mathbf{E}(\mathbf{r}) = (E_x, E_y, 0)$, and

$$\frac{\partial H}{\partial x} = -\epsilon\frac{dE_y}{dt}, \quad \frac{\partial H}{\partial y} = \epsilon\frac{dE_x}{dt},$$

$$\frac{\partial E_y}{\partial x} - \frac{\partial E_x}{\partial y} = -\frac{dH}{dt}. \tag{6}$$

We note that the equation corresponding to the E_z-polarized mode [Eq. (5)] is the so-called "scalar wave equation." In the long wavelength limit, the wave velocity for the scalar wave is the same in all directions and depends only on the average dielectric constant. Therefore the effective ϵ is trivial for the E_z-polarized mode and does not require an elaborate calculation. For the H_z-polarized mode [Eq. (6)], the situation is similar to the 3D case where the effective ϵ can only be obtained via a numerical calculation. For the H_z-polarized mode, the wave velocity generally depends on the propagation direction, unless we have an isotropic system (random or cubic). The effective ϵ will also be direction dependent. The following results refer to the effective ϵ of the H_z-polarized mode, unless otherwise specified.

1. Ordered structures

As a test case, we considered a chessboard structure which consists of alternating square patches of high and low dielectrics of $\epsilon = 10$ and 1, respectively. The unit cell has 128×128 grid points and contains four squares, two with $\epsilon = 10$ and two with $\epsilon = 1$. The initial field is a plane wave of $\mathbf{k} = (0.1,0)\frac{2\pi}{a}$, and the simulation was run for 320 000 steps at $0.001a/c$ per time step. The effective ϵ is found to be 3.162. The effective ϵ of this case is known exactly; it is $\epsilon_{\text{eff}} = \sqrt{\epsilon_1\epsilon_2} = \sqrt{10} = 3.1623$, and agrees with the numerical result.

2. Two-component disordered structures

We considered two cases in which the microstructure is disordered and uncorrelated. In the first case, we considered a two-component system, with $\epsilon = 5$ and 15, respectively. We tiled a 192×192 two-dimensional grid, such that each grid point is generated randomly, with equal probability of being either $\epsilon = 5$ or 15. The area averaged ϵ is found to be 10.043, and normalized standard deviation 0.248. The initial field is chosen to be a plane wave with $\mathbf{k} = (0.1,0)\frac{2\pi}{a}$ and the simulation was run for a total of 1×10^6 steps at a time interval of $0.0015a/c$. The effective ϵ is found to be 8.67. If the 2D system is exactly invariant with respect to the interchange of the two constituent components, the reciprocity theorem gives $\epsilon_{\text{eff}} = \sqrt{\epsilon_1\epsilon_2} = 8.66$, in good agreement with the simulation.

In the second case, we tiled a 192×192 grid such that each point is generated as a random number with average $\epsilon \sim 10$ and normalized standard deviation ~ 0.2. The initial fields correspond to a plane wave with $\mathbf{k} = (0.05,0)2\pi/a$. The time step was chosen to be $0.001a/c$

and a total of 500 000 steps was executed. We made two runs; the $\langle\epsilon\rangle$ and normalized standard deviation for the first simulation are 9.9523 and 0.2023, respectively, and for the second run they are 9.9575 and 0.2013. The effective dielectric constant was found to be 8.831 and 8.842 for the two simulation runs. The ratio $\epsilon_{\text{eff}}/\langle\epsilon\rangle$ for the two cases is 8.887 and 8.888, respectively. In two dimensions, it can be shown that up to second order in the normalized standard deviation $\epsilon_{\text{eff}}/\langle\epsilon\rangle = 1 - \frac{1}{2}\int d\mathbf{r}[\boldsymbol{\epsilon}(\mathbf{r}) - \langle\epsilon\rangle)^2/\langle\epsilon\rangle^2$, which could be regarded as the Herring formula in two dimension. This formula gives $\epsilon_{\text{eff}}/\langle\epsilon\rangle$ values of 0.899 for both cases, again in reasonable agreement with numerical results.

3. *Arbitrary structures*

In order to show that the present method can handle systems with arbitrary structures, we created one basically by freehand drawing. The structure is shown in Fig. 4. The dielectric constants for the black and the white domains are 13 and 1, respectively, with the black domain occupying 54.63% of the total area. The area averaged dielectric constant is 7.556. We used periodic boundary conditions and a mesh of 128 × 128 points to discretize the unit cell. This system does not have any symmetry, and so it has different wave velocities in different directions. To probe the effective ϵ in the x and the y directions, we used plane waves with $\mathbf{k}$ vectors $(0.1, 0)\frac{2\pi}{a}$ and $(0, 0.1)\frac{2\pi}{a}$, respectively. We used a time step of $0.001a/c$ and a total of 2×10^6 steps. In this case, we have no known results to compare with and so as a control calculation we calculated the effective dielectric constant for the E_z-polarized wave, and we found the same value of 7.56 for both directions, in good agreement with the area averaged ϵ. For the H_z-polarized wave, the ϵ_x and ϵ_y are different and they are found to be 3.78 and 4.27, respectively. We should remark that there is no easy way to compute the effective dielectric constant of such systems. We can get an estimate using the Bruggeman theory, which is a reasonably good approximation in situations where the different components are equal in importance. In two dimensions and for a two-component system, the Bruggeman equation can be written in the form

$$(1-f)\frac{\epsilon_1 - \epsilon_{\text{eff}}}{\epsilon_1 + \epsilon_{\text{eff}}} + f\frac{\epsilon_2 - \epsilon_{\text{eff}}}{\epsilon_2 + \epsilon_{\text{eff}}} = 0, \qquad (7)$$

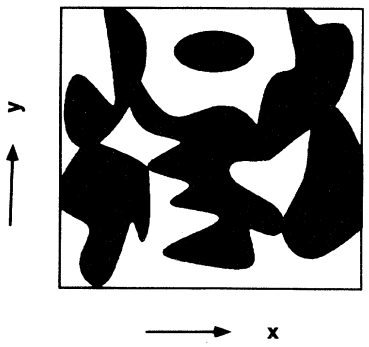

FIG. 4. The 2D motif of the arbitrary structure.

where $\epsilon_1 = 1$ and $\epsilon_2 = 13$ and $f = 0.5463$ is the area fraction for ϵ_2. Equation (7) gives $\epsilon_{\text{eff}} = 4.2$, in reasonable agreement with the numerical results.

V. STRUCTURES WITH DEFECTS

Since the complexity of this method scales like N^1, it is applicable to systems that require large cells to simulate, such as the defect states caused by structural defects in photonic crystals. This method can also give the spectral intensities at a particular point in real space. In fact, the results we have shown so far come from summing up the contributions from the individual sampling points in real space. The counterpart in electronic structure calculations is called the local density of states. This information can sometimes be very useful, as will be illustrated below.

As an example, we considered a case in which we have a photonic crystal in a stacked-bar structure with 256 (4×8×8) unit cells. The structure is composed of a stack of crisscrossed rectangular rods[25] such that the rods in the second layer are rotated by 90° with respect to the first layer and the third- and fourth-layer rods are displaced half the repeat distance with respect to the first and second layer, respectively. The system repeats itself every four layers. Details of the structure can be found elsewhere.[25] Such an arrangement of dielectric material supports a full photonic gap. In our calculation, the rods are of square cross sections ($\frac{1}{3}a \times \frac{1}{3}a$, where a is the distance between the rods). The dimension of the supercell used for the simulation is $4a \times 8a \times (16/3)a$. We introduced a structural defect by cutting away a section of length $2a$ of one of the rods that is orientated along the y direction. Each unit cell is divided into a 12×12×8 grid, and we run for a total of 80 000 time steps, with each time interval $0.003a/c$. The initial $\mathbf{H}$ field is chosen to be a random field. We impose periodic boundary conditions (which is basically equivalent to repeating the defect every 256 unit cells). We obtained the spectral intensities for the system with the defect and also the same system without defect with exactly the same initial and boundary conditions, and by comparing the spectral intensities we found that two peaks are introduced in the spectral gap when the structural defect is introduced. In Fig. 5, we plot the spectral intensity for one of the points located inside the defect, which clearly shows two defect states inside the photonic gap.

VI. REMARKS

Although we have used periodic boundary conditions in this article, periodic boundary conditions are not mandated in this scheme. If we have a situation in which the system is enclosed by metallic walls, we can simulate the situation by enclosing the domain of interest by boundary layers with negative ϵ, so that the EM waves become evanescent. The flexibility of imposing different boundary conditions is the advantage of using a real space approach in general, and is not specific to our formulation.

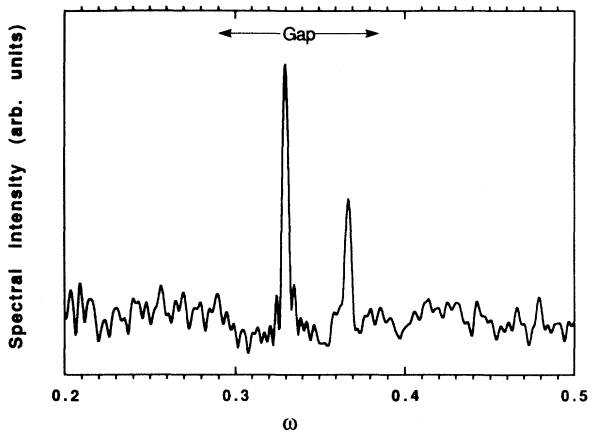

FIG. 5. The spectral intensity of one point located within the defect.

In contrast, Fourier space methods mandate the use of periodic boundary conditions and frequently large artificial periodic supercells are needed to emulate situations when the system is not periodic.

The same formulation should also be applicable to elastic waves in an inhomogeneous medium. With modest modification, the same technique can be used to study the propagation of EM waves in the presence of a source.[26]

This method can also give spectral intensities at a particular point in real space, as illustrated in the defect calculation. It will be convenient for identifying surface or interface modes. If we choose a Fourier space approach (such as plane waves), we can of course use the same technique of mapping out surface or interface states from standard electronic calculations (i.e., by solving for the eigenvalue problem and looking for states with frequencies in the gap of the bulk projected bands and which have wave amplitudes localized on the surface or interface layers). However, with the present approach, it is possible to locate the existence of such modes by just comparing the local densities of states for the points at the boundary and the points that are deep inside the bulk.

In the present work, we have considered the frequency of the normal modes, but the method can also provide information about the field distributions. Since we already have the time development of the field intensities $\phi(\mathbf{r},t)$, the field distributions for the modes at a particular frequency $\phi(\mathbf{r},\omega)$ can in principle be obtained by a Fourier transform.

ACKNOWLEDGMENTS

We thank Dr. P. Sheng for discussions on finite difference methods, and X. D. Wang for discussions on predictor-corrector algorithms. We also thank Dr. Q. M. Li and Dr. M. Sigalas for discussions. Ames Laboratory is operated for the U.S. Department of Energy by Iowa State University under Contract No. W-7405-ENG-82. This work is supported by the Director of Energy Research, Office of Basic Energy Sciences, the Advanced Energy Projects, and the Office of Scientific Computing as part of the High Performance Computing and Communication Initiative, including a grant of computer time on the Cray computers at NERSC at the Lawrence Livermore Laboratory, and on the Paragon at Oak Ridge. This work was also made possible in part by the Scalable Computing Laboratory which is funded by Iowa State University and Ames Laboratory.

[1] E. Yablonovitch, Phys. Rev. Lett. **58**, 2059 (1987); see also *Photonic Band Gaps and Localization*, edited by C.M. Soukoulis (Plenum, New York, 1993); and also numerous articles in J. Opt. Soc. Am. B. **10**, 208 (1993).

[2] E. Yablonovitch, T.J. Gmitter, and K.M. Leung, Phys. Rev. Lett. **67**, 2295 (1991); K.M. Ho, C.T. Chan, and C.M. Soukoulis, *ibid.* **65**, 3152 (1990); H.S. Sozuer and J.W. Haus, J. Opt. Soc. Am. B **10**, 296 (1993); E. Ozbay, A. Abeyta, G. Tuttle, M. Tringides, R. Biswas, C.T. Chan, C.M. Soukoulis, and K.M. Ho, Phys. Rev. B **50**, 1945 (1994); C.T. Chan, S. Datta, K.M. Ho, and C.M. Soukoulis, *ibid.* **50**, 1988 (1994). The above references are for three dimensions. Photonic gaps also exist in 2D structures. See, e.g., R.D. Meade, K.D. Brommer, A.M. Rappe, and J.D. Joannopoulos, Appl. Phys. Lett. **61**, 495 (1992); P. Villeneuve and M. Piche, Phys. Rev. B **46**, 4969 (1992); M. Philal, A. Shambrook, A.A. Maradudin, and P. Sheng, Opt. Commun. **80**, 199 (1991).

[3] K.M. Leung and Y.F. Liu, Phys. Rev. Lett. **65**, 2646 (1990); Z. Zhang and S. Satpathy, *ibid.* **65**, 2650 (1990); K.M. Ho, C.T. Chan, and C.M. Soukoulis, *ibid.* **65**, 3152 (1990); C.T. Chan, K.M. Ho, and C.M. Soukoulis, Mod. Phys. Lett. B **6**, 139 (1992).

[4] X.D. Wang, X.G. Zhang, Q.L. Yu, and B.N. Harmon, Phys. Rev. B **47**, 4161 (1993).

[5] J.B. Pendry and A. MacKinnon, Phys. Rev. Lett. **69**, 2772 (1992).

[6] N. Stefanou, V. Karathanos, and A. Modinos, J. Phys. Condens. Matter **4**, 7389 (1992).

[7] R.D. Meade, A.M. Rappe, K.D. Brommer, J.D. Joannopoulos, and O.L. Alerhand, Phys. Rev. B **48**, 8434 (1993).

[8] See, e.g., X.P. Li, R.W. Nunes, and D. Vanderbilt, Phys. Rev. B **47**, 10 891 (1993); M.S. Daw, *ibid.* **47**, 10 895 (1993); F. Mauri, G. Galli, and R. Car, *ibid.* **47**, 9973 (1993).

[9] In many cases, the Fourier transform is actually performed during the simulation to avoid storing the data on the disk.

[10] R. Alben, M. Blume, H. Krakauer, and L. Schwartz, Phys. Rev. B **12**, 4090 (1975); A. MacKinnon, in *The Recursion Method and Its Applications*, edited by P.G. Pettifor and D.L. Weaire (Springer-Verlag, Berlin, 1984), p. 84.

[11] C.Z. Wang, C.T. Chan, and K.M. Ho, Phys. Rev. B **40**, 3390 (1989).

[12] K.S. Yee, IEEE Trans. Antennas Propag. **AP-14**, 302 (1966).

[13] In principle, the spatial derivatives can be calculated to the full precision allowed by the grid if we impose periodic boundary conditions by performing fast Fourier transform (FFT) from $\mathbf{H}(\mathbf{r})$ to $\mathbf{H}(\mathbf{k})$, and then obtain $\mathbf{k}\times\mathbf{H}(\mathbf{k})$ and inverse FFT back to real space to get $\nabla \times \mathbf{H}$. Since FFT scales like $N \ln(N)$, the algorithm is still basically linear. A FFT on a $64\times64\times64$ grid can be accomplished in about 0.2 s on a 64-node N-cube2 machine [D. Turner (private communication)]. Using FFT's to find $\nabla \times \mathbf{H}$ takes six FFT's, plus some overhead to calculate $\mathbf{k} \times \mathbf{H}_\mathbf{k}$ (and the same for $\mathbf{E}$), so that it takes approximately a few seconds for each time step, and a long simulation run is not impossible. The problem with FFT on parallel machines is that the code loses "portability" since the FFT routines that are optimized on one class of machine perform poorly on others, and it is difficult to optimize the FFT routine if the dimensions are not powers of 2 on those machines.

[14] See, e.g., W.H. Press, S.A. Teukolsky, W.T. Vetterling, and B.P. Flannery, *Numerical Recipes in Fortran*, 2nd ed. (Cambridge University Press, Cambridge, England, 1992).

[15] C.T. Chan, K.M. Ho, and C.M. Soukoulis, Europhys. Lett. **16**, 563 (1991).

[16] There is no formal requirement that the $\mathbf{E}$ and $\mathbf{H}$ fields have to share the same grid. Instead of putting the $\mathbf{E}$ and the $\mathbf{H}$ fields on the same grid, we put them in a "staggered" formation, with the $\mathbf{H}$ grid points occupying one sublattice and the $\mathbf{E}$ grid points occupying another sublattice. If the $\mathbf{E}$ and $\mathbf{H}$ fields are defined on the same grid points, the spatial derivatives for the finite difference equations are obtained from points that are $2d$ apart (d is the distance between adjacent grid points); while for a staggered grid of the same density the spatial derivatives are obtained from points that are at a distance d apart. The staggered grid is thus better in spatial resolution.

[17] We should emphasize that the expansion in $\mathbf{G}$ space here is just a convenient way to impose the condition $\nabla \cdot \mathbf{H} = 0$. It is very different from the plane wave expansion method in which the number of $\mathbf{G}$ vectors used determines the accuracy and the computation time. In the present approach, the computation effort is not determined by the initial field. The number of $\mathbf{G}$ vectors used is usually small, and they are not intended to represent faithfully the eigenfunctions of the normal modes. All we need is to make sure that the initial field has nonzero projections onto the eigenstates we try to find. The $\mathbf{G}$'s here are the $\mathbf{G}$'s of the primitive unit cell, not the conventional cell.

[18] For some $\mathbf{k}$ points, we have summed up all the grid points. There is no observable difference in the results when compared with 64 randomly selected points.

[19] See, e.g., R. Landauer, in *Electrical Transport and Optical Properties of Inhomogeneous Media*, edited by J.C. Garland and D.B. Tanner, AIP Conf. Proc. No. 40 (AIP, New York, 1978).

[20] D.A.G. Bruggeman, Ann. Phys. (Leipzig) **24**, 636 (1935).

[21] J.C.M. Garnett, Philos. Trans. R. Soc. London **203**, 385 (1904).

[22] See, e.g., D.J. Bergman, in *Electrical Transport and Optical Properties of Inhomogeneous Media* (Ref. 19).

[23] R. Tao, Z. Chen, and P. Sheng, Phys. Rev. B **41**, 2417 (1990); L.C. Shen, C. Liu, J. Korringa, and K.J. Dunn, J. Appl. Phys. **67**, 7071 (1990); D.J. Bergman and K.J. Dunn, Phys. Rev. B **45**, 13 262 (1992); S. Datta, C.T. Chan, K.M. Ho, and C.M. Soukoulis, *ibid.* **48**, 14 936 (1993).

[24] C. Herring, J. Appl. Phys. **31**, 1939 (1960). We note that Herring's formulas are derived for conductivities, but effective conductivity and effective dielectric constant satisfy the same equations.

[25] K.M. Ho, C.T. Chan, C.M. Soukoulis, R. Biswas, and M. Sigalas, Solid State Commun. **89**, 413 (1994).

[26] A.R. McGurn, A.A. Maradudin, and Ping Sheng, Opt. Commun. **91**, 175 (1992).